Available online at www.sciencedirect.com
SCIENCE DIRECT
Journal of Chromatography B, 831 (2006) 236–247
JOURNAL OF CHROMATOGRAPHY B
www.elsevier.com/locate/chromb

Optimized PCR fragments for heteroduplex analysis of the whole human mitochondrial genome with denaturing HPLC

Michael Wulfert *, Christoph Tapprich, Norbert Gattermann

Department of Hematology, Oncology and Clinical Immunology, Heinrich-Heine-University, Düsseldorf, Germany

Received 5 September 2005; accepted 8 December 2005
Available online 10 January 2006

Abstract

Denaturing high pressure liquid chromatography (dHPLC) is an efficient method for discovery of unknown mutations by heteroduplex analysis of PCR fragments. For comprehensive mutation scanning of the whole 16.569 bp human mitochondrial genome, we developed a set of 67 primer pairs defining overlapping PCR fragments that are well suited for heteroduplex analysis. The aim of our optimization efforts was to ensure that point mutations are detectable at every nucleotide position of each amplicon. Some GC-rich regions of mitochondrial DNA (mtDNA) were found to have unfavourable melting profiles in all possible amplicons, therefore requiring GC-clamps at the end of one or both oligonucleotide PCR primers. Following detection of a heteroduplex pattern by dHPLC, our primers can also be employed for DNA sequencing to identify the underlying mutation. In case of heteroplasmic mutations with a low proportion of mutant mtDNA, a fragment collector is useful to recover the heteroduplex peak, which contains mutant and wildtype DNA molecules in a 1:1 ratio.

Keywords: Mitochondrial disease; Mitochondrial DNA; Mutation discovery; Heteroplasmy; Heteroduplex analysis; Denaturing HPLC; dHPLC

1. Introduction

It has been suggested that the progressive decline in mitochondrial function during ageing is due to the accumulation of acquired mutations in mitochondrial DNA [1–4]. Numerous studies have also shown that somatic mtDNA mutations are present in many different tumour types [5,6], but the importance of these mutations to the development of cancer remains uncertain.

Our interest in mitochondrial DNA stems from the possible involvement of mtDNA mutations in myelodysplastic syndromes (MDS) [7,8]. This group of clonal bone marrow disorders, some of which transform into overt leukemia, has an unclear etiology. The incidence of myelodysplastic syndromes is strongly age-related, with a peak incidence at 65–70 years [9]. Mitochondria of bone marrow cells in MDS often show ultrastructural abnormalities, including pathological iron accumulation in the mitochondria of erythroblasts (ringed sideroblasts). We have put forward a hypothesis that explains mitochondrial iron overload on the basis of a respiratory chain defect, likely attributable to mtDNA mutations [10]. In order to detect clonally expanded mtDNA mutations in the bone marrow of patients with MDS, we needed a scanning technique more economical than whole mitochondrial genome resequencing. Therefore, we turned to heteroduplex analysis with denaturing HPLC. To render mutation discovery as complete as possible, we optimized a set of overlapping PCR fragments for heteroduplex analysis.

2. Materials and methods

2.1. Heteroduplex analysis

Discovery of point mutations by heteroduplex analysis is based on the following principle: if a PCR product contains a mixture of wild-type and mutant DNA, heat denaturation of the amplified material followed by renaturation will not only allow reannealing of the perfectly matched, fully complementary strands (homoduplexes), but will also allow the formation of heteroduplexes, which have a pair of non-fitting bases (mismatch) at one position.

Abbreviations: dHPLC, denaturing high pressure liquid chromatography; TEAA, triethylammoniumacetate; T_{ann}, annealing temperature in PCR

* Corresponding author. Tel.: +49 211 81 18649; fax: +49 211 81 18853.
E-mail address: wulfert@med.uni-duesseldorf.de (M. Wulfert).

1570-0232/$ – see front matter © 2005 Elsevier B.V. All rights reserved.
doi:10.1016/j.jchromb.2005.12.024

Since a nucleotide mismatch reduces the thermodynamic stability of double stranded DNA, heteroduplexes have a lower melting temperature than homoduplexes. At a certain temperature, homoduplexes are still double-stranded while heteroduplexes are already partially denatured. At that temperature, the two DNA species can be separated by dHPLC because their binding to the dHPLC column differs. The difference in melting temperature between homo- and heteroduplexes is strongly dependent on the nucleotide sequence of the respective DNA fragment. Therefore, length and position of DNA fragments must be chosen quite carefully to favour large differences in melting temperatures, thus enabling all possible point mutations to be detected.

2.2. dHPLC

Denaturing HPLC [11] was performed with the WAVE-System (Transgenomic, Crewe, UK). Its central component is the DNASep® Cartridge (Transgenomic, Crewe, UK), a column (4.6 mm diameter, 50 mm length) containing alkylated nonporous poly(styrene-divinylbenzene) particles of 2–3 μm in diameter, which effectuate the conformation-dependent separation of nucleic acids by means of ion-pair reversed-phase liquid chromatography [12]. Two buffers were used for dHPLC analysis to form a solvent gradient: Buffer A contains 100 mM triethylammonium acetate pH 7.0 (TEAA; Transgenomic, Crewe, UK), buffer B 100 mM TEAA pH 7.0 and 25% acetonitrile (Lichrosolv®, Merck, Darmstadt, Germany). Solvent gradients were chosen according to the length and temperature-dependent melting behaviour of the PCR fragments (see tables). After each run the column was washed for 30 s with 75% acetonitrile (buffer W).

2.3. Samples

Bone marrow aspirates and blood samples were obtained for diagnostic purposes, and spare material was stored at −20 °C. From 200 μl of thawed material, DNA was extracted using the QIAamp® DNA Blood Mini Kit (Qiagen, Hilden, Germany) according to the manufacturers instructions.

2.4. PCR with heteroduplex formation

PCR reactions (50 μl) were performed in a GeneAmp 9600 PCR system (Perkin Elmer Cetus/Applied Biosystems, Langen, Germany) with 1× buffer (supplied with polymerase), 40 pmol of each primer (MWG, Ebersberg, Germany), 20 nmol of each nucleotide triphosphate (New England Biolabs, Frankfurt am Main, Germany), 1 unit VENT polymerase (New England Biolabs, Frankfurt am Main, Germany), and about 10 ng whole DNA. After an initial denaturing step of 4 min at 95 °C, 35 cycles were performed, with denaturing at 94 °C for 1 min, annealing at 49–59 °C (depending on primer pairs, T_{ann} in Tables 1 and 2) for 1 min, and elongation at 72 °C for 1 min. The last elongation step of the PCR was extended to 8 min. PCR products were then denatured again at 95 °C for 1 min, and finally cooled down to 4 °C to allow heteroduplex formation through hybridization. 10 μl of each PCR product was visualized in a 2% agarose gel. Depending on the result, 3–10 μl (usually 5 μl) of PCR product was subsequently used for each injection into the dHPLC column.

2.5. Primer design

Primer design was supported by OLIGO® 5.0 primer analysis software (National Biosciences Inc., Plymouth, USA). We chose primers of generous length (25 nucleotides) because VENT polymerase has a 3′-5′ proof-reading exonuclease activity on single stranded DNA which may lead to shortening of primers during PCR. This approach had a favourable effect on amplification efficiencies.

2.6. Melting profiles

Melting profiles were calculated using WAVE-Maker 3.4.4 software (Transgenomic, Crewe, UK). For each base pair of a PCR fragment, this program displays the probability to be in a closed configuration under the conditions used in the dHPLC, calculated for up to three different temperatures. A calculation for more than three temperatures and different solvent conditions is available at http://www.biophys.uni-duesseldorf.de/local/POLAND/poland.html. A mismatch should become visible on dHPLC analysis if a temperature increase by 1 K reduces the pairing probability at the respective nucleotide position by at least 40%. Melting temperatures are not much different between neighbouring nucleotides because DNA melts in cooperative domains. Therefore, analysis at one or two temperatures is sufficient for most PCR fragments. However, some GC-rich regions pose a problem because they do not have melting profiles suitable for dHPLC in any of the possible PCR fragments. This requires the incorporation of GC-clamps to stabilize the fragment at one or both ends, in order to achieve a more even melting profile (Fig. 1).

3. Results

3.1. PCR fragments

We designed 67 primer pairs defining overlapping PCR fragments that cover the entire human mitochondrial genome (Table 1). If primer design was straightforward and melting profiles were favourable for dHPLC analysis (e.g. in the region of COX genes), we chose relatively long PCR fragments of >400 bp. However, for DNA extracted from paraffin embedded tissues, long PCR fragments are hard to amplify. Therefore, we constructed alternative, shorter fragments for some of the genes (Table 2).

We tested our PCR fragments using samples with known nucleotide polymorphisms or somatic mutations previously identified in our laboratory. For polymorphisms, DNA was extracted from blood samples of five young adults with different ethnic backgrounds (Germany, Portugal, Cameroon, Colombia, and South Korea). Their mitochondrial genomes were sequenced by a commercial laboratory (SeqLab, Göttingen, Germany). The

Table 1
67 overlapping PCR fragments suitable for dHPLC analysis and covering the whole mitochondrial genome

Fragment	F-primer[a] R-primer[a]	Primer lengths (bp)	Primer positions[b]	PCR-length (bp)	T_{ann} (PCR) (°C)	Visibility	T_{WAVE} (°C)	WAVE buffer[c] A (%)
KR 81a	5′-AAA AAG TCT TTA ACT CCA CCA TTA G-3′ 5′-GTG GCT TTG GAG TTG CAG TTG ATG T-3′	25 25	15.962–15.986 16.259–16.235	298	59	15.987–16.031 16.032–16.234	56 59	48–36 51–39
KR 82a	5′-AAA ACC CCC TCC CCA TGC TTA CAA G-3′ 5′-ACC AGA TGT CGG ATA CAG TTC ACT T-3′	25 25	16.180–16.204 16.505–16.481	326	59	16.205–16.355 16.356–16.465	60 62	49–37 54–42
KR 83a	5′-TGA AAT CAA TAT CCC GCA CAA GAG T-3′ 5′-GAT GAG GCA GGA ATC AAA GAC AGA T-3′	25 25	16.413–16.437 150–126	307	59	16.438–74	61	50–38
KR 84a	5′-cCG Ggg Gcc C′TC CAT GCA TTT GGT ATT TTC GTC TG-3′ 5′-GcG Cgg cgg gcg g′TA GGA TGA GGC AGG AAT CAA AGA CA-3′	35 38	10∼42–66 13∼153–129	135	55	67–128	63	57–45
KR 85a	5′-CCG GAG CAC CCT ATG TCG CAG TAT C-3′ 5′-ggc ccG ggg cCc GG′T TAG GCT GGT GTT AGG GTT CTT TGT-3′	25 39	104–128 14∼385–361	296	59	129–294 295–360	58 61	49–37 5543
KR 86a	5′-CCG Cgc Cc′G GCC ACA GCA CTT AAA CAC ATC TCT-3′ 5′-AGG CTA AGC GTT TTG AGC TGC ATT G-3′	33 25	8∼322–346 794–770	481	59	347–769	58	44–32
mrR 91a	5′-ATC AAA AGG AAC AAG CAT CAA GCA C-3′ 5′-TAT CGA TTA CAG AAC AGG CTC CTC T-3′	25 25	741–765 1.220–1.196	480	59	971–1.195 766–970	58 60	45–33 49–37
mrR 92a	5′-ACT CAA AGG ACC TGG CGG TGC TTC A-3′ 5′-CAC TTA CCA TGT TAC GAC TTG TCT C-3′	25 25	1.162–1.186 1.576–1.552	415	59	1.187–1.465	60	49–37
mrR 93a	5′-gGc ggg Ccg g′GA GTA GAG TGC TTA GTT GAA CAG GG-3′ 5′-CCg Ccg cgc ggg cGC Gcg ′GGG GTT TTA GTT AAA TGT CCT TTG A-3′	35 43	10∼1.440–1.464 18∼1.534–1.510	123	57	1.465–1.509	62	57–45
mrR 94a	5′-AGA GTA GAG TGC TTA GTT GAA CAG G-3′ 5′-GGT AAA TGG TTT GGC TAA GGT TGT C-3′	25 25	1.439–1.463 1.733–1.709	295	59	1.505–1.708	59	50–38
mrR 95a	5′-CAA CTT ACA CTT AGG AGA TTT CAA C-3′ 5′-cgg gcc ′TAC AAG GGG ATT TAG AGG GTT CTG T-3′	25 31	1.628–1.652 6∼2.084–2.060	463	57	1.653–2.059	59	51–39
mrR 96a	5′-TAC CGA GCC TGG TGA TAG CTG GTT G-3′ 5′-ATA CTG GTG ATG CTA GAG GTG ATG T-3′	25 25	1.998–2.022 2.531–2.507	534	59	2.023–2.320 2.321–2.506	56 58	45–33 49–37
mrR 97a	5′-Ggg gCc CGG C′AA ATC TTA CCC CGC CTG TTT ACC AA-3′ 5′-CcG ggC Ccc C′GT GGA GCC ATT CAT ACA GGT CCC TA-3′	35 35	10∼2.480–2.504 10∼2.642–2.618	183	55	2.505–2.617	59	51–39
mrR 98a	5′-TAG CAT CAC CAG TAT TAG AGG CAC C-3′ 5′-ATT GAG TAT AGT AGT TCG CTT TGA C-3′	25 25	2.517–2.541 2.894–2.870	378	55	2.542–2.739 2.740–2.869	58 61	46–34 51–39
mrR 99a[d]	5′-CTA ACA AAC CCA CAG GTC CTA AAC T-3′ 5′-AGA ATT TTT CGT TCG GTA AGC ATT A-3′	25 25	2.762–2.786 3.389–3.365	627	57	3.262–3.364 2.841–3.261	58 61	46–34 54–42
NAD 11a	5′-GGC cgg GC′C CGG TAA TCG CAT AAA ACT TAA AAC-3′ 5′-ccG cGG C′GG GTT TTA GGG GCT CTT TGG TGA AG-3′	33 32	8∼3.246–3.270 7∼3.495–3.471	265	55	3.271–3.400 3.401–3.470	58 61	49–37 53–41
NAD 12a	5′-ATA CAA CTA CGC AAA GGC CCC AAC G-3′ 5′-GTA GAA TGA TGG CTA GGG TGA CTT C-3′	25 25	3.397–3.421 3.757–3.733	361	55	3.422–3.732	61	48–36
NAD 13a	5′-AAC TCA AAC TAC GCC CTG ATC GGC G-3′ 5′-TGT TTG TGT ATT CGG CTA TGA AGA A-3′	25 25	3.676–3.700 3.997–3.973	322	55	3.701–3.880	60	45–33

NAD 14a	5′-cGg CCC gcG GCC gcg ′ATA TGA TTT ATC TCC ACA CTA GCA G-3′ 5′-GGc Ggc ggg cgg cgc ′AAT GTT TGT GTA TTC GGC TAT GAA-3′	40 39	15∼3.856–3.880 15∼3.999–3.976	174	57	3.881–3.974	62	50–38
NAD 15a	5′-AAG GGG AGT CCG AAC TAG TCT CAG G-3′′ 5′-cgc ccg CcG c′CA TAT TTC TTA GGT TTG AGG GGG A-3	25 34	3.911–3.935 0∼4.271–4.248	371	57	3.974–4.247	58	44–32
NAD 16a	5′-GAT ATG TCT CCA TAC CCA TTA CAA T-3′ 5′-CTG CAA AGA TGG TAG AGT AGA TGA C-3′	25 25	4.214–4.238 4.515–4.491	302	49	4.240–4.325 4.326–4.490	56 59	47–35 52–40
NAD 21a	5′-GGC CCg cgC C′CC GAA AAT GTT GGT TAT ACC CTT CC-3′ 5′-cgc gcc cGC cg′G CAT GTT TAT TTC TAG GCC TAC TCA-3′	35 36	10∼4.438–4.462 11∼4.581–4.557	165	57	4.463–4.556	60	53–41
NAD 22a	5′-ATC TTT GCA GGC ACA CTC ATC ACA G-3′ 5′-gcc Gcg cG′G TAG TAT TGG TTA TGG TTC ATT GTC-3′	25 33	4.506–4.530 8∼4.738–4.714	241	57	4.531–4.713	58	49–37
NAD 23a	5′-CAA CCG CAT CCA TAA TCC TTC TAA T-3′ 5′-gcg GcG cc′G GGG GCT AGT TTT TGT CAT GTG AGA-3′	25 33	4.660–4.684 8∼4.883–4.859	232	59	4.685–4.785 4.786–4.858	56 60	50–38 57–45
NAD 24a	5′-TAG CCC CCT TTC ACT TCT GAG TCC C-3′ 5′-Gcg CGG cg′G AAC TGC TAT TAT TCA TCC TAT GTG-3′	25 33	4.792–4.816 8∼5.049–5.025	266	59	4.859–5.024	58	48–36
NAD 25a	5′-ACC AAA CCC AGC TAC GCA AAA TCT T-3′ 5′ GcG Gc′G GGT GGA TGG AAT TAA GGG TGT TA-3′	25 29	4.981–5.005 5∼5.211–5.188	236	59	5.006–5.110 5.111–5.187	57 60	50–38 56–44
NAD 26a	5′-CgC GgC CCc g′CT ACT ATC TCG CAC CTG AAA CAA G-3′ 5′-cgG cgc ggg cGG ′GGA GAT AGG TAG GAG TAG CGT GGT A-3′	34 37	10∼5.154–5.177 12∼5.489–5.465	358	57	5.300–5.380 5.179–5.464	58 60	45–33 48–36
NAD 27a	5′-CCC ACA CTC ATC GCC CTT ACC-3′ 5′-AAT TCG AAG AAG CAG CTT CAA ACC T-3′	21 25	5.448–5468 5.795–5.771	348	57	5.469–5.590 5.591–5.770	58 60	48–36 52–40
NAD 28a	5′-AGC ACC CTA ATC AAC TGG CTT CAA T-3′ 5′-TAC AAA TGC ATG GGC TGT GAC GAT A-3′	25 25	5.702–5.726 6.095–6.071	394	57	5.730–6.070	59	45–33
Cox 72b	5′-GCA TGA GCT GGA GTC CTA GGC ACA G-3′ 5′-GCT CCG GCC TCC ACT ATA GCA GAT G-3′	25 25	5.973–5.997 6.268–6.244	296	59	6.048–6.243	60	49–37
Cox 73b	5′-CCG CAT AAA CAA CAT AAG CTT CTG A-3′ 5′-GcG gcG cgg cc′G ATG GCC CCT AAG ATA GAG-3′	25 30	6.188–6.212 11∼6.389–6.371	213	59	6.238–6.370	61	53–41
Cox 74	5′-CAC CCT GGA GCC TCC GTA G-3′ 5′-TCA GGG TGA CCG AAA AAT CAG-3′	19 21	6.315–6.333 6.628–6.608	313	55	6.334–6.607 6.421–6.555	59, 61	47–35 51–39
Cox 75	5′-GCA ACC TCA ACA CCA CCT TC-3′ 5′-TCA TAT TGC TTC CGT GGA GTG-3′	20 21	6.541–6.560 6.900–6.880	360	49	6.591–6.879	59	48–36
Cox 76	5′-CGG CGT CAA AGT ATT TAG-3′ 5′-GAA TGA GCC TAC AGA TGA TAG-3′	18 21	6.851–6.868 7.280–7.260	430	49	6.871–7.259	60	47–35
Cox 77b	5′-CAT ACA CCA CAT GAA ACA TCC TAT C-3′ 5′-ATG GTT TTT CTA ATA CCT TTT TGA A-3′	25 25	7.240–7.264 7.536–7.512	297	53	7.265–7.325 7.326–7.510	56 59	48–36 52–40
Cox 21	5′-CCA AAG CTG GTT TCA AGC CAA-3′ 5′-TGG GAG GGC GAT GAG GAC T-3′	21 19	7.470–7.490 7.822–7.804	353	53	7.491–7.580 7.581–7.770	56 59	46–34 50–38

Table 1 (*Continued*)

Fragment	F-primer[a] R-primer[a]	Primer lengths (bp)	Primer positions[b]	PCR-length (bp)	T_{ann} (PCR) (°C)	Visibility	T_{WAVE} (°C)	WAVE buffer[c] A (%)
Cox 22b[d]	5′-ATG GCA CAT GCA GCG CAA GTA GGT C-3′ 5′-CGG TCG TGT AGC GGT GAA AGT GGT T-3′	25 25	7.586–7.610 8.152–8.128	567	57	7.611–8.120 7.791–8.040	58 60	42–30 46–34
Cox 23b[d]	5′-CTA ACA TCT CAG ACG CTC AGG AAA T-3′ 5′-CTA GAG GGG GTA GAG GGG GTG CTA T-3′	25 25	7.743–7.767 8.290–8.266	548	59	7.793–8.222	60	45–33
Cox 24b[d]	5′-CGG GGG TAT ACT ACG GTC AAT GCT C-3′ 5′-ccc GGc GG′T GGG GAT CAA TAG AGG GGG AAA TAG-3′	25 33	8.151–8.175 8∼8.623–8.599	481	55	8.176–8.560	58	47–35
Cox 30b[d]	5′-CTC CCT CAC CAA AGC CCA TAA AAA T-3′ 5′-GGC CTG CAG TAA TGT TAG CGG TTA G-3′	25 25	8.472–8.496 9.028–9.004	557	57	8.561–8.765 8.766–9.003	57 59	44–32 48–36
Cox 31b[d]	5′-TCA GCC TAC TCA TTC AAC CAA TAG C-3′ 5′-GGG ATT TAG CGG GGT GAT GCC TGT T-3′	25 25	8.966–8.990 9.584–9.560	619	59	8.991–9.516 9.271–9.420	58 60	43–31 46–34
Cox 32c	5′-cgg cCC gCg Gcg Gcc ′TTT TTC TTC GCA GGA TTT TTC TGA G-3′ 5′-GGc Ggc cGg cgC ′TCC TGA TGC GAG TAA TAC GGA TGT G-3′	40 37	15∼9.480–9.504 12∼9.629–9.605	177	59	9.505–9.604	62	54–42
Cox 33b	5′-TAC CAC TCC AGC CTA GCC CCT ACC C-3′ 5′-GAC CCT CAT CAA TAG ATG GAG ACA T-3′	25 25	9.510–9.534 9.988–9.964	479	59	9.601–9.963	59	47–35
Cox 34	5′-TGG CAT TTT GTA GAT GTG GTT-3′ 5′-GGG GGA TAT AGG GTC GAA-3′	21 18	9.930–9.950 10.196–10.179	267	53	9.951–10.130	56	49–37
NAD 37a	5′-GgC cgc gcC cGc gcG cCg CC′A TCT ATT GAT GAG GGT CTT ACT CTT-3′ 5′-GGG CTC ATG GTA GGG GTA AAA GGA G-3′	45 25	20∼9.972–9.996 10.293–10.269	342	55	9.997–10.268 10.141–10.240	56 59	47–35 54–42
NAD 38a	5′-ATA GAA AAA TCC ACC CCT TAC GAG T-3′ 5′-ATG AAC AGC GAT AGT ATT ATT CCT T-3′	25 25	10.149–10.173 10.594–10.570	446	59	10.211–10.569	56	47–35
NAD 41a	5′-cgg gcg ccg cgC cgG ′CAT TTA CCA TCT CAC TTC TAG GAA T-3′ 5′-cgg cGG cgc g′GT ACG TAG TCT AGG CCA TAT GTG TT-3′	40 35	15∼10.501–10.525 10∼10.740–10.716	265	59	10.526–10.670 10.671–10.715	60 62	50–38 54–42
NAD 42a	5′-GCC TAG CCC TAC TAG TCT CAA TCT C-3′ 5′-gcg gcg c′CG TGA TAG TGG TTC ACT GGA TAA GT-3′	25 32	10.690–10.714 7∼11.031–11.007	349	49	10.715–10.915 10.916–11.006	58 60	49–37 54–42
NAD 43a	5′-CCC CTC CTA ATA CTA ACT ACC TGA C-3′ 5′-gGg gcG ccc g′GT GAG CCT AGG GTG TTG TGA GTG TA-3′	25 35	10.949–10.973 10∼11.279–11.255	341	59	10.974–11.140 11.141–11.254	58 61	48–36 54–42
NAD 44a	5′-TCT ACA CCC TAG TAG GCT CCC TTC C-3′ 5′-GAG TTT GCT AGG CAG AAT AGT AAT G-3′	25 25	11.211–11.235 11.754–11.730	544	59	11.236–11.720	58	45–33
NAD 45a	5′-TCA CCG GCG CAG TCA TTC TCA TAA T-3′ 5′-TTT CTC GGT AAA TAA GGG GTC GTA A-3′	25 25	11.685–11.709 12.212–12.188	528	59	12.151–12.187 11.710–12.150	57 59	44–32 47–35
NAD 46a	5′-TTA ACC AAA ACA TCA GAT TGT GAA T-3′ 5′-TGG ACC ATG TAA CGA ACA ATG CTA C-3′	25 25	12.149–12.173 12.634–12.610	486	59	12.175–12.575	58	46–34
NAD 51a	5′-ACA CTG AGC CAC AAC CCA AAC AAC C-3′ 5′-GAT TTG CCT GCT GCT GCT AGG AGG A-3′	25 25	12.534–12.558 13.007–12.983	474	59	12.559–12.760 12.761–12.982	58 60	48–36 50–38
NAD 52a	5′-CcC gcG gGg C′CC ACA ACA AAT AGC CCT TCT AAA CG-3′ 5′-GTC ATT TTG TGT AAG GGC GCA GAC T-3′	35 25	10∼12.928–12.952 13.227–13.203	310	59	13.081–13.202 12.968–13.080	60 62	48–36 51–39

NAD 53a	5′-CTA ACA CTA TGC TTA GGC GCT ATC A-3′	25	13.162–13.186	533	53	13.187–13.650	59	45–33
	5′-GGG TTT AGT AGG GTG GGG TTA TTT T-3′	25	13.694–13.670					
NAD 54a	5′-TAA TTC TTC TCA CCC TAA CAG GTC A-3′	25	13.613–13.637	376	59	13.638–13.840	58	46–34
	5′-AGT AGG GGC AGG TTT TGG CTC G-3′	22	13.988–13.967			13.841–13.966	60	50–38
NAD 61a	5′-ACA ATC CCC TAT CTA GGC CTT CTT A-3′	25	13.942–13.966	437	59	13.967–14.241	58	47–35
	5′-AGG TAG GAT TGG TGC TGT GGG TGA A-3′	25	14.378–14.354					
NAD 62b	5′-ACC TAT TCC CCC GAG CAA TCT CAA T-3′	25	14.148–14.172	346	55	14.242–14.468	60	49–37
	5′-GGG GGA ATG ATG GTT GTC TTT GGA T-3′	25	14.493–14.469					
NAD 63a	5′-ACT CCT CAA TAG CCA TCG CTG TAG T-3′	25	14.442–14.466	163	53	14.467–14.556	56	55–43
	5′-TCT CCT ATT TAT GGG GGT TTA GTA T-3′	25	14.604–14.580					
NAD 64a	5′-AAA CCC ATA TAA CCT CCC CCA AAA T-3′	25	14.516–14.540	342	59	14.557–14.786	58	48–36
	5′-AAG GAG TGA GCC GAA GTT TCA TCA T-3′	25	14.857–14.833					
Cyb 01	5′-CGG ACT ACA ACC ACG ACC AAT-3′	21	14.684–14.704	172	49	14.705–14.809	58	53–41
	5′-GGA GTG AGC CGA AGT TTC ATC-3′	21	14.855–14.835					
Cyb 02	5′-AAC CAC TCA TTC ATC GAC CTC-3′	21	14.789–14.809	199	53	14.935–14.968	61	52–40
	5′-AGC GGA TGA TTC AGC CAT A-3′	19	14.987–14.969			14.810–14.934	63	54–42
Cyb 03	5′-CTA TTC CTA GCC ATG CAC TAC-3′	21	14.891–14.911	337	57	15.011–15.170	60	47–35
	5′-CTA GGT CTG TCC CAA TGT ATG-3′	21	15.227–15.207			14.912–15.010	62	52–40
Cyb 04	5′-AAC ATC GGC ATT ATC CTC CTG-3′	21	15.086–15.106	280	53	15.107–15.346	60	49–37
	5′-TGT TTG ATC CCG TTT CGT G-3′	19	15.365–15.347					
Cyb 05	5′-ACT TCA TCT TGC CCT TCA TT-3′	20	15.291–15.310	294	53	15.316–15.560	60	50–38
	5′-TTG TGT AGG CGA ATA GGA AAT-3′	21	15.584–15.564					
Cyb 06b	5′-CCA GAC AAT TAT ACC CTA GCC AAC C-3′	25	15.503–15.527	369	53	15.631–15.780	58	47–35
	5′-TTT GTT TTC AAT TAG GGA GAT AGT T-3′	25	15.871–15.847			15.528–15.630	60	52–40
Cyb 07a	5′-CTG AAT CGG AGG ACA ACC AGT AAG C-3′	25	15.754–15.778	286	57	15.779–15.990	57	51–39
	5′-CTT CCC CAT GAA AGA ACA GAG AAT A-3′	25	16.039–16.015					

[a] Not matching nucleotides of the GC clamps in the 5′-regions of the primers are written in lower letters.
[b] 10∼: GC clamp with 10 GC at the 5′ end of the primer, not fully matching the mitochondrial sequence.
[c] Gradient buffer A for analysis. Buffer B accordant.
[d] May be replaced by shorter PCR fragments according to Table 2.

Table 2
Additional fragments to replace long PCR-products

Fragment[d]	F-primer[a] R-primer[a]	Primer lengths (bp)	Primer positions[b]	PCR-length (bp)	T_{ann} (PCR) (°C)	Visibility	T_{WAVE} (°C)	WAVE buffer[c] A (%)
TR 88a	5′-AAA CTA CCA AAC CTG CAT TAA AAA T-3′ 5′-AGA TAG AAA CCG ACC TGG ATT ACT C-3′	25 25	2.782–2.806 3.104–3.080	323	53	2.857–3.079	60	47–35
TR 89a	5′-CCG CTA TTA AAG GTT CGT TTG TTC A-3′ 5′-TTT TCG TTC GGT AAG CAT TAG GAA T-3′	25 25	3.020–3.044 3.384–3.360	364	53	3.060–3.359	59	47–35
Cox 57a	5′-Cgg cgC gGC ggC Ccg G′ TCC TGT ATG CCC TTT TCC TAA CAC T-3′ 5′-TCG ATT GTC AAC GTC AAG GAG TCG C-3′	41 25	16∼7.698–7.722 8.008–7.984	327	55	7.723–7.983	60	46–34
Cox 58a	5′-ACT CCT ACA TAC TTC CCC CAT TAT T-3′ 5′-gGG Gcg ggc g′CG GGC CCT ATT TCA AAG ATT TTT AG-3′	25 35	7.941–7.965 10∼8.255–8.231	325	51	7.966–8.230	60	48–36
ATP 87a	5′-AAC CAA ACC ACT TTC ACC GCT ACA C-3′ 5′-ccC gCc Gcg ggG cGG′ TGT TGG TTC TCT TAA TCT TTA ACT T-3′	25 40	8.123–8.147 15∼8.350–8.326	243	51	8.148–8.325	60	52–40
ATP 88a	5′-ATT CCC CTA AAA ATC TTT GAA ATA G-3′ 5′-gcG GG′C TTT GGT GAG GGA GGT AGG TGG TAG-3′	25 30	8.225–8.249 5∼8.485–8.461	266	55	8.305–8.460	58	49–37
ATP 65a	5′-cgC gCc gcg Ccc Cgc′ CAC CCA ACT AAA AAT ATT AAA CAC A-3′ 5′-ATT TGG AGG TGG GGA TCA ATA GAG G-3′	40 25	15∼8.434–8.458 8.632–8.608	214	55	8.459–8.607	59	51–39
ATP 66a	5′-CGC CGC AGT ACT GAT CAT TCT ATT T-3′ 5′-AGG GGA TGG CCA TGG CTA GGT TTA T-3′	25 25	8.580–8.604 8.848–8.824	269	55	8.605–8.764	57	47–35
ATP 67a	5′-CTA AAG GAC GAA CCT GAT CTC TTA T-3′ 5′-GAG TAG GTG GCC TGC AGT AAT GTT A-3′	25 25	8.714–8.738 9.036–9.012	323	55	8.765–9.011	60	48–36
ATP 68a	5′-ggG GCg CgC Ccg C′ ACC CCT TAT CCC CAT ACT AGT TAT T-3′ 5′-ATG TGT TGT CGT GCA GGT AGA GGC T-3′	38 25	13∼8.931–8.955 9.205–9.181	288	55	9.068–9.180 8.956–9.067	59 61	48–36 52–40
ATP 69a	5′-GCc ggC Ccg Cgg CgC ccg cC′ ATC TTC ACA ATT CTA ATT CTA CTG A-3′ 5′ GAG TGG AAG TGA AAT CAC ATG GCT A-3′	45 25	20∼9.100–9.124 9.322–9.298	243	55	9.125–9.297	61	48–36
Cox 35a	5′-CCC TCT CAG CCC TCC TAA TGA CCT C-3′ 5′-CTC AGA AAA ATC CTG CGA AGA AAA A-3′	25 25	9.268–9.292 9.504–9.480	237	55	9.293–9.443	62	54–42
Cox 36a	5′-GAT GGC GCG ATG TAA CAC GAG AAA G–3′ 5′-TCC TGA TGC GAG TAA TAC GGA TGT G-3′	25 25	9.376–9.400 9.629–9.605	254	53	9.401–9.511	60	49–37

[a] Not matching nucleotides of the GC clamps in the 5′-regions of the primers are written in lower letters.
[b] 10∼: GC clamp with 10 GC at the 5′ end of the primer, not fully matching the mitochondrial sequence.
[c] Gradient buffer A for analysis. Buffer B accordant.
[d] TR 88a and TR 89a replaces mrR 99a, Cox 57a to Cox 36a replaces Cox 22b to Cox 31b.

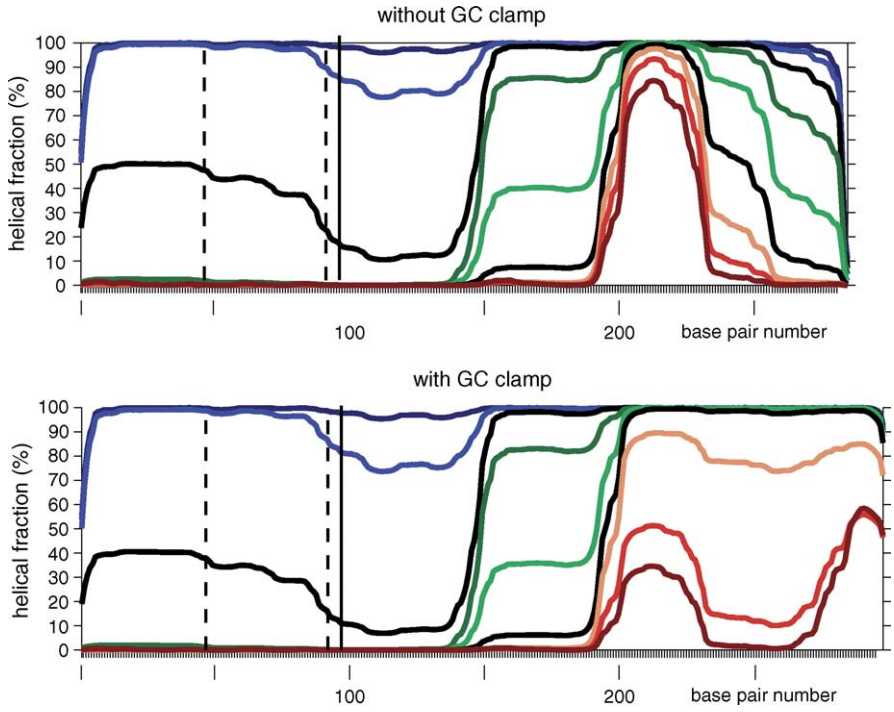

Fig. 1. Melting profiles of PCR fragment KR 85a, calculated with WAVE Maker software. For each base pair of the sequence (x-axis), the probability is given in percent (y-axis) for being in the double stranded state, at temperatures from 56 °C (blue) to 64 °C (red). The top panel, without GC clamp, shows a very stable region of the fragment (positions 200–230). The lower panel shows that, with 14 G/Cs at the 5′-end of the R-primer, stabilisation of the 5′-end of the fragment occurs, creating a larger and more even cooperative melting domain that enables thermodynamic analysis. Dashed lines indicate the positions of polymorphisms underlying the heteroduplex pattern in Fig. 2 lower panel. Solid line indicates the position of the heteroplasmic mutation relevant to Figs. 3 and 4.

polymorphisms were used for mixing experiments with mtDNA from another healthy individual. Two wild type samples and all available mutations were at least analysed at six appropriate temperatures for each PCR fragment, using an universal gradient that changed buffer A from 60 to 28% over 17 min (Table 3). An example is shown in Fig. 2. Employing the available polymorphisms in 27 PCR fragments, as well as previously identified heteroplasmic point mutations in further 23 PCR fragments, we were pleased to see that all sequence changes were detected by dHPLC analysis.

Table 3
WAVE-Gradient for PCR fragment testing (Universal gradient), used with multiple temperatures

Time (min)	Buffer A (%)	Buffer B (%)	Buffer W (%)	Description
0.0	65	35	0	Sample injection
1.0	60	40	0	Start gradient
17.0	28	72	0	End gradient
17.1	0	0	100	Start wash
18.1	0	0	100	End wash
18.2	65	35	0	Start equilibration
20.1	65	35	0	for next injection

Buffer A, 0.1 M TEAA (triethylammonium acetate); buffer B, 0.1 M TEAA, 25% acetonitrile; buffer W, 75% acetonitrile.

3.2. HPLC parameters

The heteroduplex chromatograms resulting from heteroplasmic mutations or from mixtures of polymorphic sequences were used to choose appropriate analysis temperatures for each PCR fragment (T_{WAVE}, Tables 1 and 2). They also helped to optimize other dHPLC parameters. A 6-min solvent gradient was chosen, so that the homoduplex peak will elute after 5–6 min. For sample injection at the beginning of the gradient, buffer A is increased by 5% for 0.1 min. At the end of the gradient, the column is washed with 75% acetonitrile (100% buffer W) for 0.5 min. While the wash peak is recorded by the detector (time lag between solvent pump and detector: 2 min), the column is already being equilibrated for 2 min, preparing it for the next injection. Analysis of each sample requires about 10 min (ca. 9 min for the gradient, and another minute for washing the injection system and for data processing).

As an example, the gradient programs for PCR fragment KR 85a are shown in Table 4 (left, analysis temperature 58 °C and right, analysis temperature 61 °C).

3.3. GC clamping

As already mentioned, some PCR fragments required GC clamping. An example is given in Fig. 1. Fragment KR 85a (nt 104–385) shows a GC-rich stretch of about 30 nucleotides

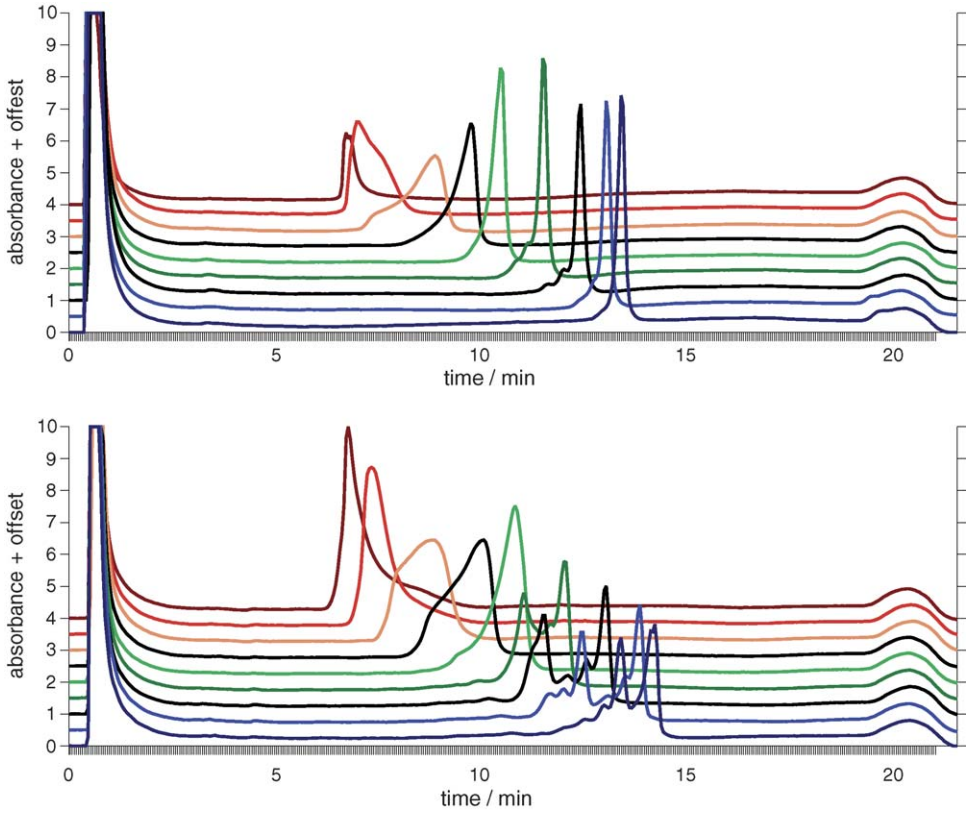

Fig. 2. dHPLC analysis of PCR fragment KR 85a at different temperatures, from 56 °C (blue) to 64 °C (red). Upper panel: wildtype; lower panel: mixture of samples characterized by two polymorphisms that create mismatches at positions 47 and 92 of this fragment (see Fig. 1). Heteroduplex patterns are clearly detectable over a broad range of temperatures. For routine analysis, 58 and 61 °C (black lines) were chosen.

where basepairs did not melt even at high temperatures. Adding a GC clamp of 14 nucleotides at the 5′ end of the reverse primer significantly altered the melting behaviour, allowing the recalcitrant GC-rich sequence to become part of a larger and less stable cooperative melting domain, thereby enabling mismatches to be detected at temperatures of 62–63 °C.

3.4. *"Shoulders" in wildtype homoduplex peaks*

PCR amplification is not free of errors, which may contribute, like acquired mutations, to the formation of heteroduplex molecules, thereby causing "shoulders" or small additional peaks on dHPLC analysis. To avoid or diminish those artefacts, we used a "high-fidelity" DNA polymerase featuring 3′-5′ exonuclease activity which can remove falsely incorporated nucleotides. The error rate of high-fidely polymerases is about ten times smaller than that of Taq polymerase. We found that normal shoulders are best distinguished from conspicuous findings if homologous PCR fragments from 10 to 20 different samples are run through the column in succession. Since the normal chromatogram has a characteristic pattern for each PCR fragment, deviations from that pattern are conspicious. In Fig. 3, for example, sample 12 shows a small heteroduplex peak that differs from the normal shoulder seen in the other samples.

Table 4
WAVE gradients for PCR fragment KR 85a as an example

KR 85a, 58 °C				KR 85a, 61 °C			
Time (min)	Buffer A (%)	Buffer B (%)	Buffer W (%)	Time (min)	Buffer A (%)	Buffer B (%)	Buffer W (%)
0.0	54[b]	46	0	0.0	60[b]	40	0
0.1	49[a]	51	0	0.1	55[a]	45	0
6.1	37[a]	63	0	6.1	43[a]	57	0
6.2	0	0	100	6.2	0	0	100
6.7	0	0	100	6.7	0	0	100
6.8	54[b]	46	0	0.0	60[b]	40	0
8.8	54[b]	46	0	0.0	60[b]	40	0

Buffer A, 0.1 M TEAA (triethylammonium acetate); buffer B, 0.1 M TEAA, 25% acetonitrile; buffer W, 75% acetonitrile.
[a] This values are mentioned as WAVE buffer A in Tables 1 and 2.
[b] This values are always 5% higher than the buffer A value at 0.1 min, buffer B accordant.

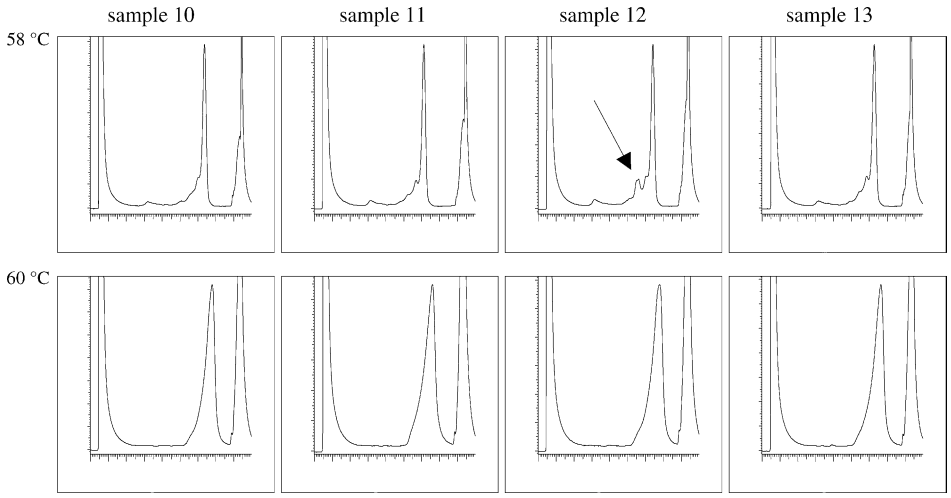

Fig. 3. Chromatograms of PCR fragment KR 85a from four different individuals. Detector output at 260 nm shows a peak at 0,5 min (on the far left) containing all UV-absorbing material not retained by the column, e.g. nucleotides (for changing solvent conditions, see Table 4). The peak on the far right represents genomic DNA that leaves the column during the wash step at the end of each run. The PCR fragment of interest elutes at around 6 min. All chromatograms are scaled to show the fragment peak at maximum hight. Upper row: dHPLC at 58 °C; lower row: dHPLC at 61 °C. Sample no. 12 shows a small additional peak (arrow) at 58 °C, which turned out to be a clonally expanded mtDNA mutation (Fig. 4). The "shoulders" seen on the left side of each homoduplex peak result from nucleotides falsely incorporated by the polymerase. These PCR errors contribute, like acquired mutations, to the formation of heteroduplex molecules.

3.5. Retrieval of heteroduplex species for DNA sequencing of "low-level" mutations

Heteroduplex findings were always confirmed by repeat PCR and dHPLC. If mutant DNA represented around 50% of the PCR product, mutations were easily confirmed and identified by direct DNA sequencing. In case of <30% mutant DNA, sequencing may yield ambiguous results not clearly distinguishable from background noise. To circumvent this problem, we used a fraction collector (FC) to elute the heteroduplex peak, which represents an equimolar mixture of mutant and wildtype DNA strands [13]. For each sample, 12 fractions were collected, with a collection time of 6 s and a volume of 150 μl, respectively. These fractions, containing TEAA, acetonitrile, and the eluted DNA, can be entered into PCR amplifications without further preparation. After PCR amplification of the heteroduplex fraction, the presence of mutant and wildtype DNA in a ratio of 50:50 can be confirmed by re-analysis of the PCR product in another dHPLC. The PCR product is then suitable for mutation identification through DNA sequencing using our forward and reverse primers. Fig. 4 demonstrates how the small heteroduplex peak shown in Fig. 3 is further processed according to this approach.

4. Discussion

We developed a set of primer pairs defining 67 overlapping PCR fragments suitable for heteroduplex analysis of the entire human mitochondrial genome with denaturing HPLC. We took special care to facilitate mutation detection at all nucleotide positions.

The availability of optimized PCR fragments has several advantages.

First, the mitochondrial genome has GC-rich regions which require stabilization with GC clamps at one or both ends of certain fragments in order to make them amenable to analysis by thermodynamic methods. Such GC clamps are incorporated into our primers. MtDNA fragments created by long-range PCR followed by restriction enzyme digestion [14,15] cannot harness the favourable effect of GC clamps.

Second, after finding a heteroduplex peak, a suspected mutation must be identified by DNA sequencing. For this purpose, we can use the same primers as employed for PCR amplification of the respective mtDNA fragment. Methods creating fragments by restriction enzymes need extra primers for DNA sequencing.

Third, we can enrich low-level heteroplasmic mtDNA mutations through retrieval of heteroduplex peaks by means of a fraction collector, followed by PCR amplification of the eluted heteroduplex DNA. Again, this enrichment is only possible if there are PCR primers available for the respective fragment.

Fourth, mtDNA fragments created by restriction enzymes may produce closely adjacent wild-type peaks on dHPLC, which may in some cases obscure a heteroduplex peak or at least hinder the detection of low-level heteroplasmic mutations.

If mtDNA fragments for dHPLC analysis are produced with the help of restriction enzymes, fewer PCR fragments are needed. However, machine time is not saved, since aiming at completeness of mutation detection requires those restriction fragments to be analysed at several temperatures.

With our method, heteroduplex analysis of the entire mtDNA of 20 individuals requires 67 PCR amplifications and about 2000 sample injections into the HPLC column. This takes 2–4 weeks, depending on whether the WAVE system is in continuous operation.

For just one individual, the mitochondrial genome can be scanned within 48 h: 1 day for PCR amplifications and another day for dHPLC analyses. However, besides being less economical, this approach renders the interpretation of results more difficult because chromatograms cannot be compared to a row

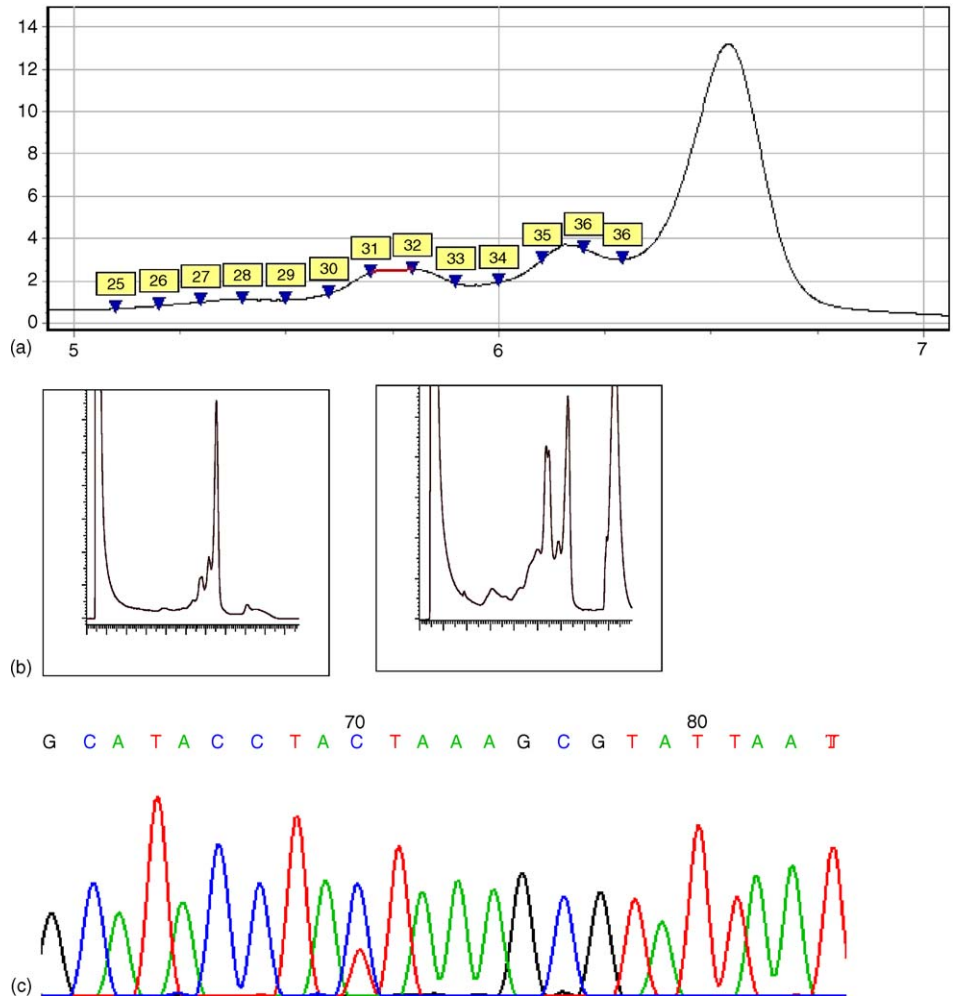

Fig. 4. Enrichment of low-level heteroplasmic mutations. a) dHPLC of PCR fragment KR 85a of sample no. 12, analysed at 58 °C. The heteroduplex peak, containing equimolar amounts of wildtype and mutant PCR product, was collected. The contents of vial 31, representing the red coloured part of the chromatogram, was reamplified. b) on the left: the original chromatogram (same as in a); on the right: reamplification and repeat dHPLC of the small heteroduplex peak (vial 31) confimed a clear heteroduplex pattern, with a proportion of mutant mtDNA suitable for DNA sequencing. c) Results of DNA sequencing: a mutation C/T is clearly detectable at position 70 of the amplicon, which corresponds to position 198 in the control region of mtDNA [16,17]. C198T has been reported as a polymorphism [18]. The DNA sequence of this highly polymorphic stretch of mtDNA shows four additional (homoplasmic) deviations from the Cambridge reference sequence [16,17], all representing well-known inherited polymorphisms [18]: A189G (here position 61), T195C (67), T204C (76), and G207A (79).

of homologous fragments from other individuals analysed under identical conditions.

Using our optimized PCR fragments, we performed heteroduplex analysis of mitochondrial DNA from bone marrow cells of patients with myelodysplastic syndromes. In 58 of 104 patients, we identified 111 clonally expanded somatic mutations of mtDNA (manuscript in preparation). The mutations are scattered over the whole mitochondrial genome, which is not unexpected. Mitochondrial DNA mutations in different sites can have very similar effects, because all mitochondrial genes contribute to a functioning respiratory chain.

Acknowledgements

This work was supported by Deutsche Krebshilfe, Mildred Scheel Stiftung, grant no. 10-2147-Ga 2.

We are grateful to the five colleagues from different continents who donated a blood sample for identification of their mtDNA polymorphisms, and to Monika Pooten for outstanding technical assistance.

References

[1] D.C. Wallace, Annu. Rev. Genet. 39 (2005) 359.
[2] G. Hofhaus, M. Berneburg, M. Wulfert, N. Gattermann, Exp. Physiol. 88 (2003) 167.
[3] A. Trifunovic, A. Wredenberg, M. Falkenberg, J.N. Spelbrink, A.T. Rovio, C.E. Bruder, M. Bohlooly, Y.S. Gidlöf, A. Oldfors, R. Wibom, J. Törnell, H.T. Jacobs, N.G. Larsson, Nature 429 (2004)417.
[4] G.C. Kujoth, A. Hiona, T.D. Pugh, S. Someya, K. Panzer, S.E. Wohlgemuth, T. Hofer, A.Y. Seo, R. Sullivan, W.A. Jobling, J.D. Morrow, H. Van Remmen, J.M. Sedivy, T. Yamasoba, M. Tanokura, R. Weindruch, C. Leeuwenbrugh, T.A. Prolla, Science 309 (2005) 481.
[5] J.S. Penta, F.M. Johnson, J.T. Wachsman, W.C. Copeland, Mutat. Res. 488 (2001) 119.
[6] J.S. Carew, P. Huang, Mol. Cancer 1 (2002) 9 (www.molecular-cancer.com/content/1/1/9).
[7] N. Gattermann, Leukemia Res. 24 (1999) 141.

[8] N. Gattermann, Leukemia 18 (2004) 18.
[9] D.P. Steensma, A. Tefferi, Leuk. Res. 27 (2003) 95.
[10] P.L. Greenberg, N.S. Young, N. Gattermann, Hematology (Am Soc. Hematol. Educ. Prog.) (2002) 136.
[11] A. Kuklin, K.Y. Munson, D. Gjerde, R. Haefele, P. Taylor, Genet. Test. 1 (1997) 201.
[12] W. Xiao, P.J. Oefner, Hum. Mut. 17 (2001) 439.
[13] P. Emmerson, J. Mayard, S. Jones, R. Butler, J.R. Sampson, J.P. Cheadle, Hum. Mut. 21 (2003) 112.
[14] B.J.C. van den Bosch, R.F.M. de Coo, H.R. Scholte, J.G. Nijland, R. van den Bogaard, M. de Visser, C.E.M. de Die-Smulders, H.J.M. Smeets, Nucleic Acids Res. 28 (2000) e89.
[15] A. Bayat, J. Walter, H. Lambe, J.S. Watson, J.K. Stanley, M. Marino, M.W.J. Ferguson, W.E.R. Ollier, Plast. Reconstr. Surg. 115 (2005) 134.
[16] S. Anderson, A.T. Bankier, B.G. Barrell, M.H.L. de Bruijn, A.R. Coulson, J. Drouin, I.C. Eperon, D.P. Nierlich, B.A. Roe, F. Sanger, P.H. Schreier, A.J.H. Smith, R. Staden, I.G. Young, Nature 290 (1981) 457.
[17] R.M. Andrews, I. Kubacka, P.F. Chinnery, R.N. Lightowlers, D.M. Turnbull, N. Howell, Nat. Genet. (1999) 147.
[18] M.C. Brandon, M.T. Lott, K.C. Nguyen, S. Spolim, S.B. Navathe, P. Baldi, D.C. Wallace, Nucleic Acids Res. 33 (2005) D611, Database issue.